Iranian Journal of Electrical and Electronic Engineering

Journal Homepage: ijeee.iust.ac.ir

Research Paper

Adaptive Dynamic Sliding Mode Algorithm for BDFIG Control

M. Ehsani*, A. Oraee**(C.A), B. Abdi*, V. Behnamgol***, and S. M. Hakimi*

Abstract: A novel nonlinear controller is proposed to track active and reactive power for a Brushless Doubly-Fed Induction Generator (BDFIG) wind turbine. Due to nonlinear dynamics and the presence of parametric uncertainties and perturbations in this system, sliding mode control is employed. To generate a smooth control signal, dynamic sliding mode method is used. Uncertainties bound is not required in the suggested algorithm, since the adaptive gain in the controller relation is used in this study. Convergence of the sliding variable to zero and adaptive gain to the uncertainty bound are verified using Lyapunov stability theorem. The proposed controller is evaluated in a comprehensive simulation on the BDFIG model. Moreover, output performance of the proposed control algorithm is compared to the conventional and second order sliding mode and proportional-integral-derivative (PID) controllers.

Keywords: Brushless Doubly-Fed Induction Machine, Dynamic Sliding Mode Control, Adaptive Gain, Uncertainty.

Nomenclature

PV	Photovoltaic
Pw, Cw	Power winding, control winding
V_r, V_{sc}, V_{sp}	Voltage of Rotor, Cw, Pw
$\Phi_r, \Phi_{sc}, \Phi_{sp}$	Flux of Rotor, Cw, Pw
I_r, I_{sc}, I_{sp}	Current of Rotor, Cw, Pw
R_r, R_{sc}, R_{sp}	Resistance of Rotor, Cw, Pw
P_c, P_p	Number of pole pair of Cw, Pw
$\omega_r, \omega_{sc}, \omega_{sp}$	Electrical angular velocities of Rotor, Cw, Pw
L_r, L_{sc}, L_{sp}	Self-inductance of Rotor, Cw, Pw
M_c, M_p	Mutual inductance Cw, Pw
P_{sp}, Q_{sp}	Active and reactive power of Pw

Iranian Journal of Electrical and Electronic Engineering, 2023. Paper first received 24 Jan 2022, revised 28 Sep 2022, and accepted 19 Oct 2022

*The authors are with the Department of Electrical Engineering and Renewable Energy Research Centre, Damavand Branch, Islamic Azad University, Tehran, Iran.
E-mails: ehsani.Mohsen.bbb@gmail.com, babakabdii@gmail.com, and Sm_hakimi@damavandiau.ac.ir.
**The author is with Sajjad University of Technology, Mashhad, Iran.
E-mails: ashknaz.Oraee@gmail.com.
***The author is with Malek Ashtar University of Technology, Tehran, Iran.
E-mails: vahid_behnamgol@mut.ac.ir.
Corresponding Author: A. Oraee.
https://doi.org/10.22068/IJEEE.19.1.2405

1 Introduction

IN recent years, due to climate change much attention has been given to exploring various economic clean power generation methods. This has led to an increase in investigating alternative energy sources such as renewable energy. Renewable energy systems have made significant progress recently, due to the advances in converter technology and upgrades to control strategies. Furthermore, the Brushless Doubly-fed Induction Generator (DFIG) has been greatly investigated due to its higher performance at variable wind speeds [1].

Brushless DFIG, like other AC machines, are controlled by scalar and vector methods. Novelty of the vector control method is the independency of machine parameters used in [2] for Brushless DFIG prototypes.

When modelling systems, uncertainties may arise due to possible unmodulated dynamics and neglected nonlinear effects in the linearization of equations as well as possible perturbations. To control these systems, Sliding Mode Control (SMC)

theory can be used, which is specially known for nonlinear and uncertain systems [3]. This control method has been used for various wind turbines. In [4] an integrated sliding mode controller is used to eliminate speed errors and counteract the effects of disturbances in a brushless doubly-fed machine used in a wind turbine. In [5] Sliding mode control method has been used to simultaneously achieve smooth synchronization with the network and flexible adjustment of power when connected to the network. In [6] sliding mode control has been used to control Brushless DFIG wind turbine for both grid and island modes. In addition, predictive SMC was utilized in [7] to control active and reactive power of this system and controller gains are optimized by Particle Swarm Optimization method. SMC is also used for a Brushless DFIG in [8]. Due to the use of sign function in input relationships of the first-order sliding mode control, an oscillation occurs in the control signal, which is called chattering phenomenon [9]. Chattering is an undesired obstacle for implementing first-order SMC. Therefore, several methods have been proposed to eliminate the effect of chattering to achieve a smooth SMC control signal. A simple method to eliminate the effect of chattering is to replace a discontinuous function with a continuous approximation in boundary layer.

Another method to eliminate chattering is High-order SMC (HOSMC). This type of SMC for a DIFG was employed in [10]. The well-known second-order SMC, super twisting was implemented to control Brushless DFIG in [1] and [11]. Disadvantage of HOSMC is that they have complex calculations to prove stability, and their computational volume is much larger than the first-order method.

To deface the chattering effects, dynamic sliding mode control (DSMC) can be used. In the DSMC method, the sliding variable is defined in such a way that by deriving it, the first derivative of the control input appears. Then the derivative of the control input is considered as a new control input and is designed [12]. In this method, since the derivative of control input signal is designed directly, the control signal passes through an interceptor applied to the system, therefore there are no high frequency fluctuations present [13] and [14]. The dynamic sliding mode method provides better stability and performance in the presence of uncertainties. [15]. In addition, dynamic integral sliding mode was analyzed in [16]. References [17] and [18] present the principles of controller design by fractional order dynamic sliding mode control, which has proved to reduce the effects of chattering in control signal. In [19] improved dynamic sliding mode with higher speed in reaching phase was introduced and in [20] DSMC with resistance capability in the presence of mismatched incompatible uncertainty has been used for a DC-DC converter. In [21] an observer-based DSMC is presented using a proportional-integral sliding surface. Although this method is advantageous, however due to the PI consideration of the sliding surface, effects of chattering is higher in comparison with the conventional method. To solve this problem, the sign function is replaced by the saturation at the input signal of the discontinuous function. Furthermore, this method of removing chattering effects, which is similar to continuous approximation in a narrow boundary layer, leads to a reduction in accuracy levels and does not prove stability.

Another design challenge in SMC is to manage system uncertainties. For this purpose, the adaptive sliding mode control (ASMC) has been introduced, where switching gain is employed to manage unknown uncertainties.

The adaptive sliding mode control basis is presented in [22-25]. Although in these studies the need for uncertainty upper bound was investigated by adaptive method, but the problem of chattering has not been resolved.

The aim of this study is to use a robust nonlinear method to control active and reactive powers of the Brushless DFIG producing a smooth control signal without knowing the upper bound of uncertainties. Therefore, the combined adaptive dynamic sliding mode control for Brushless DFIG is proposed.

The structure of the article is as follows. In the second part, the mathematical model of BDFIG is described. In Section 3, the adaptive dynamic SMC theory is explained and used to control this type of Brushless DFIG wind turbine. The result of simulations is provided in Section 4. Finally, conclusions are presented in Section 5.

2 BDFIG Dynamics Model

In this section, the Brushless DFIG equations are expressed in d-q coordinates [1] and [26]. The stator power winding is rotating at an angular velocity ω_{sp} and the rotor angular velocity is as follows:

$$\omega_r = \frac{\omega_{sc} \pm \omega_{sp}}{P_c + P_p} \tag{1}$$

The relationship between flux, voltage and current of the power and control sections of the stator and rotor is given by:

$$
\begin{aligned}
v_{sp} &= R_{sp} I_{sp} + \frac{d}{dt}\Phi_{sp} + j\omega_{sp}\Phi_{sp}\theta \\
v_{sc} &= R_{sc} I_{sc} + \frac{d}{dt}\Phi_{sc} \\
&\quad + j\left(\omega_{sp} - \left(p_p + p_c\right)\omega_r\right)\Phi_{sc} \\
v_r &= R_r I_r + \frac{d}{dt}\Phi_r + j\left(\omega_{sp} - p_p\omega_r\right)\Phi_r
\end{aligned} \tag{2}
$$

And the flux relation can be expressed as:

$$
\begin{aligned}
\Phi_{sp} &= L_{sp} I_{sp} + M_p I_r \\
\Phi_{sc} &= L_{sc} I_{sc} + M_c I_r \\
\Phi_r &= L_r I_r + M_c I_{sc} + M_p I_{sp}
\end{aligned} \tag{3}
$$

The electromagnetic torque is:

$$
\begin{aligned}
T_{em} &= \frac{3}{2} P_p M_p \left(I_{sp}^q I_r^d - I_{sp}^d I_r^q\right) \\
&\quad - \frac{3}{2} P_c M_c \left(I_{sc}^q I_r^d - I_{sc}^d I_r^q\right)
\end{aligned} \tag{4}
$$

The stator active and reactive power expressions are:

$$
\begin{aligned}
P_{sp} &= \frac{3}{2}\left(v_{sp}^d I_{sp}^d + v_{sp}^q I_{sp}^q\right) \\
Q_{sp} &= \frac{3}{2}\left(v_{sp}^q I_{sp}^d + v_{sp}^d I_{sp}^d\right)
\end{aligned} \tag{5}
$$

The following can be extracted from Eq. (3):

$$
\begin{aligned}
I_{sp} &= \frac{\Phi_{sp} - M_p I_r^d}{L_{sp}} \\
I_r &= \frac{\Phi_r - M_p I_{sp} - M_c I_{sc}}{L_r}
\end{aligned} \tag{6}
$$

And we conclude from Eqs. (3) and (6):

$$
\begin{aligned}
I_{sp} &= \frac{L_r}{L_{sp}L_r - M_p^2}\Phi_{sp} + \frac{M_p}{L_{sp}L_r - M_p^2}\Phi_r \\
&\quad + \frac{M_c M_p}{L_{sp}L_r - M_p^2} I_{sc}
\end{aligned} \tag{7}
$$

The substitution of Eq. (6) in Eqs. (3) and (4) gives:

$$
\begin{aligned}
P_{sp} &= \frac{3}{2} V_{sp}\left(\lambda_5 \Phi_{sp}^q - \lambda_4 \Phi_r^q + \lambda_3 I_{sc}^q\right) \\
Q_{sp} &= \frac{3}{2} V_{sp}\left(\lambda_5 \Phi_{sp}^d - \lambda_4 \Phi_r^d + \lambda_3 I_{sc}^d\right)
\end{aligned} \tag{8}
$$

$$
\begin{aligned}
\lambda_1 &= \frac{L_{sp} M_c}{L_r L_{sp} - M_p^2}, \quad \lambda_2 = L_{sc} - \frac{L_{sp} M_c^2}{L_r L_{sp} - M_p^2}, \\
\lambda_3 &= \frac{M_c M_p}{L_r L_{sp} - M_p^2}, \quad \lambda_4 = \frac{M_p}{L_r L_{sp} - M_p^2}, \\
\lambda_5 &= \frac{L_r}{L_r L_{sp} - M_p^2},
\end{aligned} \tag{9}
$$

It can be concluded from the equations above that the dynamic relationship between control winding current and voltages in the d–q axis is determined as follows:

$$
\begin{aligned}
V_{sc}^d &= R_{sc} I_{sc}^d \left(\frac{d}{dt}\left(\lambda_1 \Phi_r^d + \lambda_2 I_{sc}^d\right)\right. \\
&\quad \left. - \omega_{sc}\left(\lambda_1 \Phi_r^q + \lambda_2 I_{sc}^q - \lambda_3 \Phi_{sp}^q\right)\right) \\
V_{sc}^q &= R_{sc} I_{sc}^q \left(\frac{d}{dt}\left(\lambda_1 \Phi_r^q + \lambda_2 I_{sc}^q\right)\right. \\
&\quad \left. + \omega_{sc}\left(\lambda_1 \Phi_r^d + \lambda_2 I_{sc}^d - \lambda_3 \Phi_{sp}^d\right)\right)
\end{aligned} \tag{10}
$$

3 Controller Design

In this section, principle of adaptive dynamic sliding mode control theory is explained. Later, this controller method is used to control active and reactive power of a Brushless DFIG wind turbine.

3.1 Adaptive Dynamic Sliding Mode Control

Consider a nonlinear system as:

$$\dot{x} = f(x) + g(x)u + d(t) \tag{11}$$

where $x \in X \subset R^n$ is a vector of state variables, $u \in R$ is a control input and $f(x) \in R^n$ is a nonlinear function vector-field. Assuming:

A1. The sliding variable $s = s(x,t) \in R$ is defined in such a way that if it is set to zero, the system Eq. (11) will behave desirable.

A2. The relative degree of the sliding variable *s(x, t)* with respect to the control input is equal to one, and the internal dynamics of system Eq. (11) are stable. Therefore, the input–output dynamics can be presented as:

$$
\begin{aligned}
\dot{s} &= \frac{\partial s}{\partial t} + \frac{\partial s}{\partial x} f(x) + \frac{\partial s}{\partial t} g(x)u \\
&= a(x,t) + b(x,t)u
\end{aligned} \tag{12}
$$

A3. The function $b(x,t) \in R$ is certain and the function $a(x,t) \in R$ is expressed as:

$$a(x,t) = \bar{a}(x,t) + d \tag{13}$$

where $\bar{a}(x,t)$ and d are known and uncertain parts of the $a(x,t)$, respectively. Also it is assumed that uncertainty is bounded with $|d| \le L_d$.

$$a(x,t) = \bar{a}(x,t) + d \tag{13}$$

The problem is to design the control input *u* in the presence of uncertainty *d* to bring *s* to zero.

The standard first-order sliding mode control is able to bring the sliding variable to zero in a finite time. In conventional sliding mode control the control input is selected as follow:

$$u = \frac{1}{b(x,t)}\left[-\bar{a}(x,t) - ksign(s)\right] \tag{14}$$

in which k is the reaching term. By defining the candidate Lyapunov function as $V = \frac{1}{2}s^2$, the following condition must be established for the finite time stabilization of the sliding variable:

$$\dot{V} = s\dot{s} \le -\eta\left|s\right| \tag{15}$$

where η is a strictly positive constant, which implies that:

$$t_r \le \frac{\left|s(0)\right|}{\eta} \tag{16}$$

and t_r is the reaching time [27].

The control input of Eq. (14) contains the discontinuous function of the sign that causes chattering in the control signal. Using the simple method of continuous approximation, this control input can be replaced by the following equation:

$$u = \frac{1}{b(x,t)}\left[-\bar{a}(x,t) - ksat_{\varepsilon}(s)\right] \tag{17}$$

In the dynamic sliding mode method, the discrete part of the controller is placed under an integrator. Therefore, chattering of the control signal will be less [17]. To explain this method, consider the following nonlinear system:

$$\begin{cases} \dot{x}_1 = x_2 \\ \dot{x}_2 = f(x) + g(x)u + d(t) \\ y = x_1 \end{cases} \tag{18}$$

Define the tracking error and the switching function as $e = y - y_d$ and $s = ce + \dot{e}$ respectively where $c > 0$. Therefore:

$$\dot{s} = f(x) + g(x)u + d(t) - \ddot{y}_d + c\dot{e} \tag{19}$$

Now the new sliding variable is defined as follows:

$$\sigma = \dot{s} + \lambda s \tag{20}$$

where $\lambda > 0$. When $\sigma = 0,\ \dot{s} + \lambda s = 0$ is asymptotically stable, therefore, $e \to 0$ and $\dot{e} \to 0$.

Stability analysis from Eq. (20), is given as follows:

$$\begin{aligned} \sigma &= \dot{s} + \lambda s \\ &= f(x) + g(x)u + d(t) - \ddot{y}_d + c\dot{e} + \lambda s \end{aligned} \tag{21}$$

Therefore:

$$\begin{aligned} \dot{\sigma} &= \dot{f}(x) + \dot{g}(x)u + g(x)\dot{u} + \dot{d}(t) \\ &\quad - \dddot{y} + c\ddot{e} + \lambda\dot{s} \\ &= \dot{f}(x) + \dot{g}(x)u + g(x)\dot{u} + \dot{d}(t) \\ &\quad - \dddot{y} + c\left(f(x) + g(x)u + d(t) - \ddot{y}_d\right) \\ &\quad + \lambda\left(f(x) + g(x)u + d(t) - \ddot{y}_d + c\dot{e}\right) \\ &= \dot{f}(x) - (c+\lambda)\ddot{y}_d - \dddot{y}_d + \dot{d}(t) \\ &\quad + (c+\lambda)d(t) + \left(\dot{g}(x) + cg(x) + \lambda g(x)\right)u \\ &\quad + (c+\lambda)f(x) + g(x)\dot{u} + \lambda c\dot{e} \end{aligned} \tag{22}$$

Dynamic controller is selected as:

$$\begin{aligned} \dot{u} = \frac{1}{g(x)}&(-\dot{f}(x) + (c+\lambda)\ddot{y}_d + \dddot{y}_d \\ &-\left(\dot{g}(x) + cg(x) + \lambda g(x)\right)u \\ &-(c+\lambda)f(x) - \lambda c\dot{e} - \eta\,\mathrm{sgn}(\sigma)) \end{aligned} \tag{23}$$

From Eqs. (22) and (23), it is obtained [28]:

$$\dot{\sigma} = \dot{d}(t) + (c+\lambda)d(t) - \eta\,\mathrm{sgn}(\sigma) \tag{24}$$

Considering that $\left|d(t)\right| \le L_d$, $\left|\dot{d}(t)\right| \le L_{\dot{d}}$ then, Let $\eta > L_{\dot{d}} + (c+\lambda)L_d$, therefore:

$$\begin{aligned} \sigma\dot{\sigma} &= \sigma\left(\dot{d}(t) + (c+\lambda)d(t) - \eta\,\mathrm{sgn}(\sigma)\right) \\ &= \sigma\left(\dot{d}(t) + (c+\lambda)d(t)\right) - \eta\left|\sigma\right| \\ &\le \left(L_{\dot{d}} + (c+\lambda)L_d\right)\sigma - \eta\left|\sigma\right| < 0 \end{aligned} \tag{25}$$

Determining switching gain at the control inputs Eq. (17) and Eq. (23) requires an upper bound of the uncertain part. If this parameter is not known, the adaptive sliding mode method can be used. This method has been introduced in recent years with the ability to adaptively adjust the switching gain [25]. In this method, the control input is provided Eq. (26) for the system in Eq. (12), which does not require the uncertainty upper bound.

$$\begin{cases} u = \dfrac{1}{b(x,t)}\left(-\bar{a}(x,t) - \hat{k}(t)sign(s)\right) \\ \dot{\hat{k}}(t) = k_0\left|s\right| \\ k_0 > 0 \end{cases} \tag{26}$$

Using the system control input Eq. (12) we have:

$$\begin{cases} \dot{s} = -\hat{k}(t)sign(s) + d(t) \\ \dot{\hat{k}}(t) = k_0 |s| \end{cases} \tag{27}$$

To evaluate stability of the system Eq. (27), Lyapunov function is used Eq. (28):

$$V = \frac{1}{2}s^2 + \frac{1}{2k_0}(\hat{k} - L_d)^2 \tag{28}$$

The derivative of this Lyapunov function is:

$$\begin{aligned} \dot{V} &= s\dot{s} + \frac{1}{k_0}(\hat{k} - L_d)\dot{\hat{k}} \\ &= s\left(-\hat{k}sign(s) + d(t)\right) \\ &\quad + \frac{1}{k_0}(\hat{k} - L_d)k_0|s| \\ &= -\hat{k}|s| + d(t)s + \hat{k}|s| - L_d|s| \\ &= +d(t)s - L_d|s| < 0 \end{aligned} \tag{29}$$

Therefore, s and $\hat{k} - L_d$ are stable. Using the control input Eq. (26), in addition to ensuring the convergence of the sliding variable, $\hat{k}(t)$ converges to the uncertainty bound [25]. It should be noted that the cost of not considering the upper limit of uncertainty in the proposed method is spending a certain amount of time to converge the adaptive interest to the upper limit of uncertainty.

To take advantage of producing a smooth control signal and achieve independency to uncertainty bound, combination of dynamic and adaptive methods can be used. In this case, the input control equation (23) is as follows:

$$\begin{aligned} &\dot{u} = \frac{1}{g(x)}(\chi(x,u) - \eta \,\mathrm{sgn}(\sigma)) \\ &\dot{\hat{\eta}}(t) = \eta_0|\sigma|, \qquad \eta_0 > 0 \\ &\chi(x,u) = -\dot{f}(x) + (c+\lambda)\ddot{y}_d + \dddot{y}_d \\ &\qquad\qquad -\left(\dot{g}(x) + cg(x) + \lambda g(x)\right)u \\ &\qquad\qquad -(c+\lambda)f(x) - \lambda c\dot{e} \end{aligned} \tag{30}$$

Because the control input signal is obtained by integration from Eq. (30), the oscillations of this signal will become smoother after passing through the integrator, thus preventing chattering.

3.2 ADSMC in Brushless DFIG for a Wind Turbine

The given relationship between the control winding (CW) and the power winding (PW) are obtained as follows:

$$\begin{cases} I_{sc}^{d} = \dfrac{Q_{sp}}{1.5V_{sp}^{q}\lambda_3} + \dfrac{\lambda_4}{\lambda_3}\Phi_r^d - \dfrac{\lambda_5}{\lambda_3}\Phi_{sp}^d \\ I_{sc}^{q} = \dfrac{P_{sp}}{1.5V_{sp}^{q}\lambda_3} + \dfrac{\lambda_4}{\lambda_3}\Phi_r^q \end{cases} \tag{31}$$

We have:

$$\begin{cases} I_{sc}^{d\_ref} = \dfrac{Q_{sp}^{ref}}{1.5V_{sp}^{q}\lambda_3} + \dfrac{\lambda_4}{\lambda_3}\Phi_r^d - \dfrac{\lambda_5}{\lambda_3}\Phi_{sp}^d \\ I_{sc}^{q\_ref} = \dfrac{P_{sp}^{ref}}{1.5V_{sp}^{q}\lambda_3} + \dfrac{\lambda_4}{\lambda_3}\Phi_r^q \end{cases} \tag{32}$$

Now based on standard sliding mode control theory, sliding variables can be introduced as:

$$\begin{cases} S(P_{sp}) = \left(I_{sc}^{q} - I_{sc}^{q\_ref}\right) \\ S(Q_{sp}) = \left(I_{sc}^{d} - I_{sc}^{d\_ref}\right) \end{cases} \tag{33}$$

Then, we have:

$$\begin{cases} \dot{S}(P_{sp}) = \left(\dot{I}_{sc}^{q} - \dot{I}_{sc}^{q\_ref}\right) \\ \dot{S}(Q_{sp}) = \left(\dot{I}_{sc}^{d} - \dot{I}_{sc}^{d\_ref}\right) \end{cases} \tag{34}$$

According to Eq. (10), the derivative of currents $\left(I_{sc}^{\dot{d}}, I_{sc}^{\dot{q}}\right)$ can be calculated as follows:

$$\begin{cases} \dfrac{d}{dt}(I_{sc}^{d}) = \dfrac{V_{sc}^{d}}{\lambda_2} - \dfrac{R_{sc}}{\lambda_2}I_{sc}^{d} \\ \qquad + \dfrac{\omega_{sc}}{\lambda_2}(\lambda_1\Phi_r^q + \lambda_2 I_{sc}^{q}) - \dfrac{\lambda_1}{\lambda_2}\dot{\Phi}_r^d \\ \dfrac{d}{dt}(I_{sc}^{q}) = \dfrac{V_{sc}^{q}}{\lambda_2} - \dfrac{R_{sc}}{\lambda_2}I_{sc}^{q} \\ \qquad + \dfrac{\omega_{sc}}{\lambda_2}(\lambda_1\Phi_r^d + \lambda_2 I_{sc}^{d} - \lambda_3\Phi_{sp}^d) - \dfrac{\lambda_1}{\lambda_2}\dot{\Phi}_r^q \end{cases} \tag{35}$$

Using Eq. (35) in Eq. (34):

$$\begin{cases} \dot{S}(P_{sp}) = \dfrac{V_{sc}^{q}}{\lambda_2} - \dfrac{R_{sc}}{\lambda_2}I_{sc}^{q} \\ \qquad + \dfrac{\omega_{sc}}{\lambda_2}(\lambda_1\Phi_r^d + \lambda_2 I_{sc}^{d} - \lambda_3\Phi_{sp}^d) \\ \qquad - \dfrac{\lambda_1}{\lambda_2}\dot{\Phi}_r^q - \dot{I}_{sc}^{q\_ref} = b_P u_P + d_P(t) \\ \dot{S}(Q_{sp}) = \dfrac{V_{sc}^{d}}{\lambda_2} - \dfrac{R_{sc}}{\lambda_2}I_{sc}^{d} \\ \qquad + \dfrac{\omega_{sc}}{\lambda_2}(\lambda_1\Phi_r^q + \lambda_2 I_{sc}^{q}) \\ \qquad - \dfrac{\lambda_1}{\lambda_2}\dot{\Phi}_r^d - \dot{I}_{sc}^{d\_ref} = b_Q u_Q + d_Q(t) \end{cases} \tag{36}$$

Where:

$$b_P = \frac{1}{\lambda_2},\ u_P = V_{sc}^{\ q},\ b_Q = \frac{1}{\lambda_2},\ u_Q = V_{sc}^{\ d},$$

$$d_P(t) = -\frac{R_{sc}}{\lambda_2} I_{sc}^q + \frac{\omega_{sc}}{\lambda_2}(\lambda_1 \Phi_r^d + \lambda_2 I_{sc}^d - \lambda_3 \Phi_{sp}^d) - \frac{\lambda_1}{\lambda_2}\dot{\Phi}_r^q - \dot{I}_{sc}^{q\_ref}$$

$$d_Q(t) = -\frac{R_{sc}}{\lambda_2} I_{sc}^d + \frac{\omega_{sc}}{\lambda_2}(\lambda_1 \Phi_r^q + \lambda_2 I_{sc}^q) - \frac{\lambda_1}{\lambda_2}\dot{\Phi}_r^d - \dot{I}_{sc}^{d\_ref}\ .$$

In the convectional sliding mode control, control input is chosen as follows:

$$u_P = \frac{1}{b_P}\left[-k_P sign(S(P_{sp}))\right]$$
$$u_Q = \frac{1}{b_Q}\left[-k_Q sign(S(Q_{sp}))\right] \quad (37)$$

where $k_P = L_{d_p} + \eta_p$ and $k_Q = L_{d_Q} + \eta_Q$.

Therefore, by placing the variables, voltage of the stator control coil in the d-q coordinate system is determined as:

$$V_{sc}^{\ q} = \lambda_2\left(-\left(L_{d_P} + \eta_P\right)\mathrm{sgn}\left(I_{sc}^q - I_{sc}^{q\_ref}\right)\right)$$
$$V_{sc}^{\ d} = \lambda_2\left(-\left(L_{d_Q} + \eta_Q\right)\mathrm{sgn}\left(I_{sc}^d - I_{sc}^{d\_ref}\right)\right) \quad (38)$$

Using the continuous approximation method, controller Eq. (38) is replaced by a continuous equation such as:

$$V_{sc}^{\ q} = \lambda_2\left(-\left(L_{d_P} + \eta_P\right)sat\left(I_{sc}^q - I_{sc}^{q\_ref}\right)\right)$$
$$V_{sc}^{\ d} = \lambda_2\left(-\left(L_{d_Q} + \eta_Q\right)sat\left(I_{sc}^d - I_{sc}^{d\_ref}\right)\right) \quad (39)$$

Based on DSMC, a new dynamic switching functions is achieved using:

$$\sigma(P_{SP}) = \dot{S}(P_{sp}) + \lambda_P S(P_{sp})$$
$$\sigma(Q_{SP}) = \dot{S}(Q_{sp}) + \lambda_Q S(Q_{sp}) \quad (40)$$

Where $\lambda_P, \lambda_Q > 0$. The derivation of Eq. (39) is:

$$\dot{\sigma}(P_{SP}) = \dot{b}_P u_P + b_P \dot{u}_P + \dot{d}_P(t) + \lambda_P\left(b_P u_P + d_P(t)\right) = \beta_P \dot{u}_P + D_p$$
$$\dot{\sigma}(Q_{SP}) = \dot{b}_Q u_Q + b_Q \dot{u}_Q + \dot{d}_Q(t) + \lambda_Q\left(b_Q u_Q + d_Q(t)\right) = \beta_Q \dot{u}_Q + D_Q \quad (41)$$

Where $\beta_P = b_P$

$D_p = \dot{b}_P u_P + \dot{d}_P(t) + \lambda_P\left(b_P u_P + d_P(t)\right)$, $\beta_Q = b_Q$, and $D_Q = \dot{b}_Q u_Q + \dot{d}_Q(t) + \lambda_Q\left(b_Q u_Q + d_Q(t)\right)$.

According to adaptive dynamic sliding mode controller is given by:

$$\dot{u}_P = \frac{1}{\beta_P}\left(-\hat{\eta}_P\ \mathrm{sgn}(\sigma(P_{SP}))\right)$$
$$\dot{\hat{\eta}}_P(t) = \eta_{0P}\left|\sigma(P_{SP})\right|, \qquad \eta_{0P} > 0$$
$$\dot{u}_Q = \frac{1}{\beta_Q}\left(-\hat{\eta}_Q\ \mathrm{sgn}(\sigma(Q_{SP}))\right)$$
$$\dot{\hat{\eta}}_Q(t) = \eta_{0Q}\left|\sigma(Q_{SP})\right|, \qquad \eta_{0Q} > 0 \quad (42)$$

Therefore, by placing the variables, voltage of the stator control coil in the d-q coordinate system is determined as:

$$\dot{V}_{sc}^{\ q} = \lambda_2\left(-\hat{\eta}_P\ \mathrm{sgn}\left(\left(\dot{I}_{sc}^q - \dot{I}_{sc}^{q\_ref}\right) + \lambda_P\left(I_{sc}^q - I_{sc}^{q\_ref}\right)\right)\right)$$
$$\dot{\hat{\eta}}_P(t) = \eta_{0P}\left|\left(\dot{I}_{sc}^q - \dot{I}_{sc}^{q\_ref}\right) + \lambda_P\left(I_{sc}^q - I_{sc}^{q\_ref}\right)\right|, \quad \eta_{0P} > 0$$
$$\dot{V}_{sc}^{\ d} = \lambda_2\left(-\hat{\eta}_Q\ \mathrm{sgn}\left(\left(\dot{I}_{sc}^d - \dot{I}_{sc}^{d\_ref}\right) + \lambda_Q\left(I_{sc}^d - I_{sc}^{d\_ref}\right)\right)\right)$$
$$\dot{\hat{\eta}}_Q(t) = \eta_{0Q}\left|\left(\dot{I}_{sc}^d - \dot{I}_{sc}^{d\_ref}\right) + \lambda_Q\left(I_{sc}^d - I_{sc}^{d\_ref}\right)\right|, \quad \eta_{0Q} > 0 \quad (43)$$

4 Simulation Results

Performance of the proposed controller has been verified using MATLAB simulations and compared with PID, conventional and second order SMC methods. The required parameters are presented in Table 1. In the wind turbine management system, the controller is allowed to work from 2 seconds, and in 8 to 10 seconds, due to a voltage dip, the control algorithm is taken out of circuit and the rotor current is tracked.

Table 1 Prototype machine specifications [26].

Parameter	Value
Frame size	D180
PW pole-pairs	2
CW pole-pairs	4
Natural speed	500 rpm
Stator slots	48
Rotor slots	36
PW rated voltage	240 V (at 50 Hz)
CW rated voltage	240 V (at 50 Hz)
PW rated current	7 A
CW rated current	7 A
Rated generating torque	100 Nm
L_{sp}	0.3498 H
L_{sc}	0.3637 H
L_{spr}	0.0031 H
L_{scr}	0.0022 H
L_r	4.4521×10^{-5}H
R_{sp}	2.3 Ω
R_{sc}	4 Ω
R_r	1.2967×10^{-4}Ω
J	0.53 kgm^2
B	0.036 Nms
Rotor design	Nested-loop
Rated generating torque	100 Nm

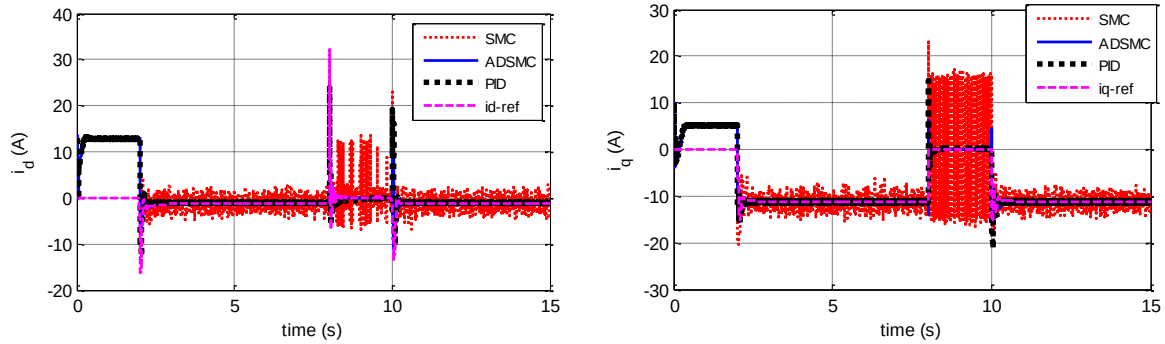

Fig. 1 Current tracking in the d-q coordinates by applying SMC, ADSMC and PID.

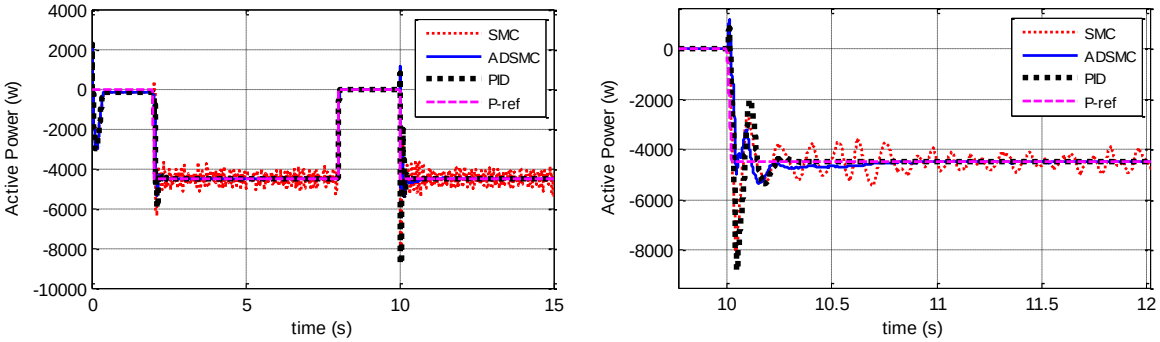

Fig. 2 Tracking active power by applying SMC, ADSMC and PID.

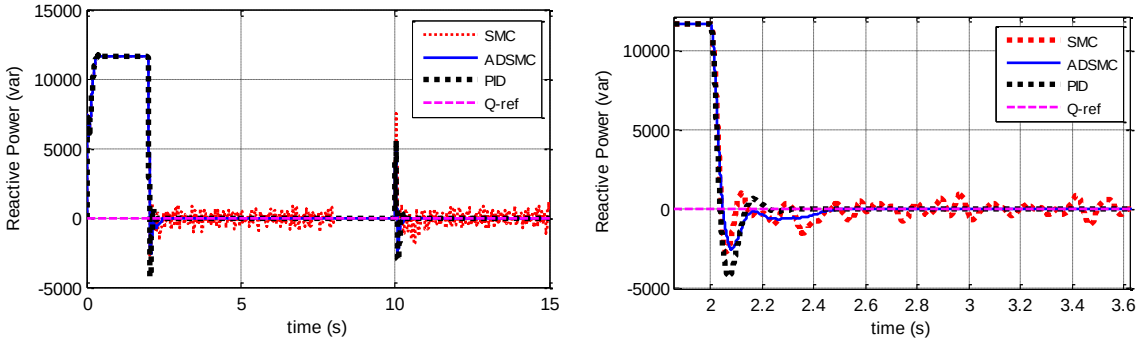

Fig. 3 Tracking the reactive power by applying SMC, ADSMC and PID.

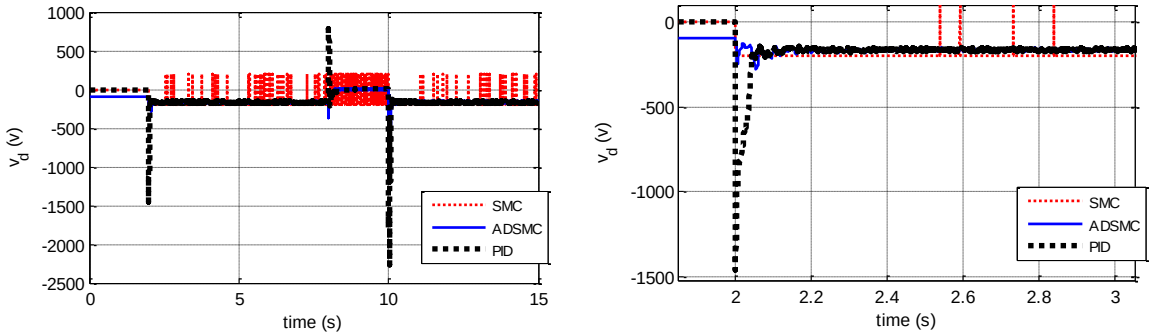

Fig. 4 Control signal along the d-axis in d-q coordinates by applying SMC, ADSMC and PID.

Figure 1 shows the current tracking in the d-q coordinates by applying SMC, ADSMC and PID controllers. According to the figures, it can be seen that all three controllers accurately track the desired current values, however the ADSMC and conventional SMC have reduced over shoots in comparison to the PID controller and chattering effects occurs in conventional SMC.

Fig. 2 and Fig. 3 show tracking of active and reactive power by applying SMC, ADSMC and PID controllers. When voltage dip is resolved and the controller is triggered, the DSMC and standard SMC have lower over shoots in comparison to the PID controller.

In Fig. 4 and Fig. 5 the control signals commanded by the SMC, the ADSMC and the PID controller are plotted. It can be seen that the standard

SMC suffers from large amount chattering effects making implementation almost impossible. However, control signal generated by the ADSMC method is smooth. By applying the control signal generated by the PID method, the system may be damaged and therefore requires saturation of the control signal. Also Fig. 6 shows the switching term gains in conventional and Adaptive DSMC methods. Finally shaft speed and torque by applying SMC, ADSMC and PID controllers are plotted in Fig. 7.

Now performance of the proposed controller has been compared with second order SMC method. Fig. 8 shows the current tracking in the d-q coordinates by applying ADSMC and SOSMC controllers. It can be seen that all three controllers accurately track the desired current values, however the ADSMC have reduced over shoots in comparison to the SOSMC controller. Chattering effects is removed using both control methods.

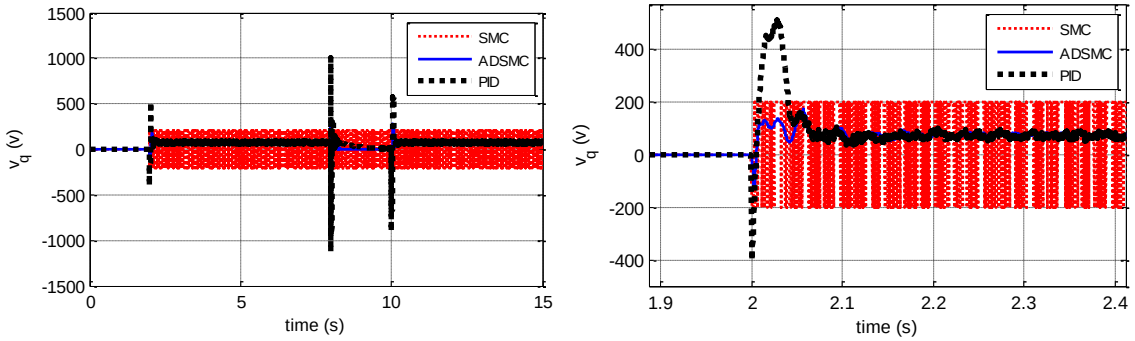

Fig. 5 Control signal along the q-axis in d-q coordinates by applying SMC, ADSMC and PID.

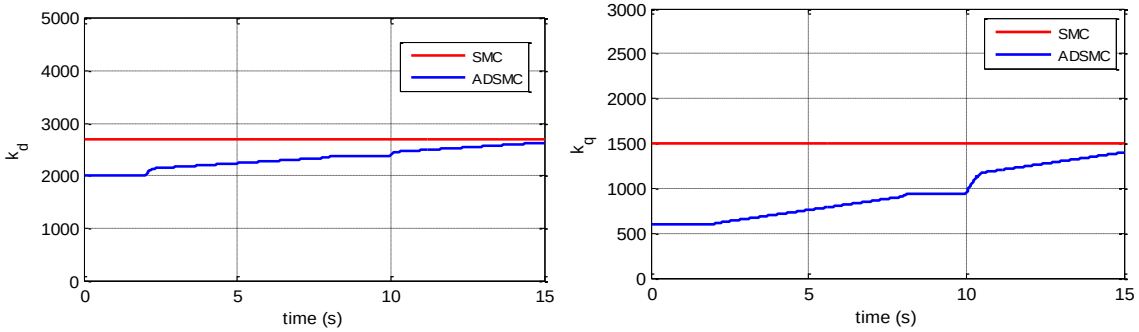

Fig. 6 Switching term gains in conventional and adaptive SMC methods.

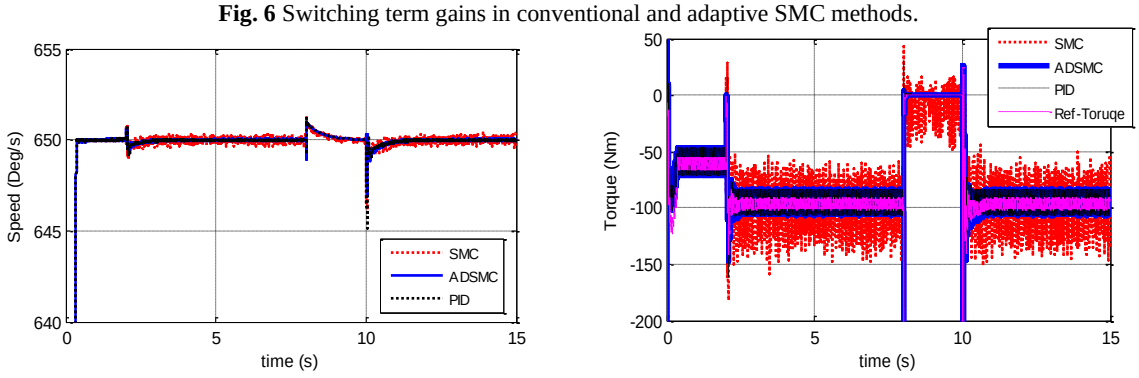

Fig. 7 Shaft speed and torque using SMC, ADSMC and PID.

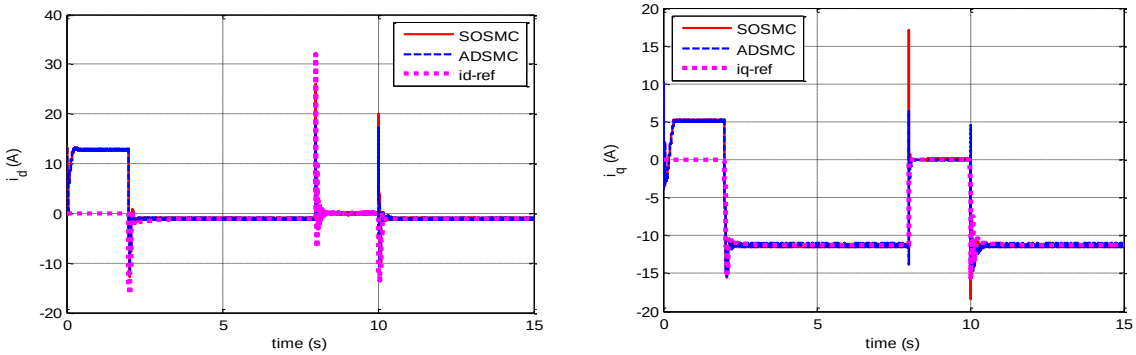

Fig. 8 Current tracking in the d-q coordinates by applying ADSMC and SOSMC.

Figures 9 and 10 show tracking of active and reactive powers by applying ADSMC and SOSMC controllers. When voltage dip is resolved and the controller is triggered, the ADSMC has lower over shoots in comparison to the SOSMC controller.

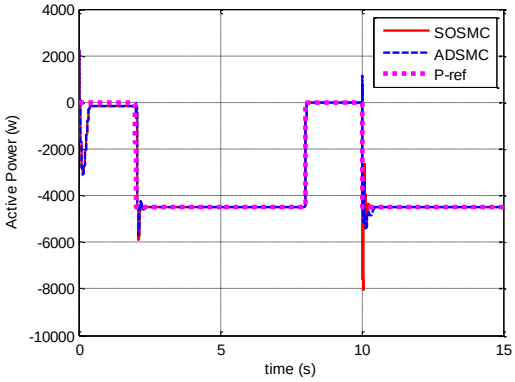

Fig. 9 Tracking the active power by applying ADSMC and SOSMC.

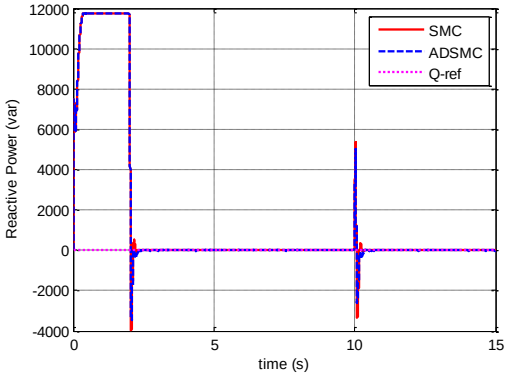

Fig. 10 Tracking the reactive power by applying ADSMC and SOSMC.

In Fig. 11 and Fig. 12 the control signals commanded by the ADSMC and the SOSMC controllers are plotted. It can be seen, both controllers have no chattering effects making implementation possible. The control signal generated by ADSMC method has lower amplitude in comparison with SOSMC method. It should be noted that in the proposed method there is no need to know the upper limit of uncertainty.

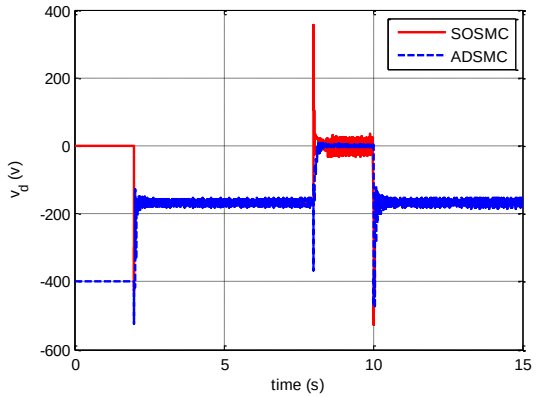

Fig. 11 Control signal along the d-axis in d-q coordinates by applying ADSMC and SOSMC.

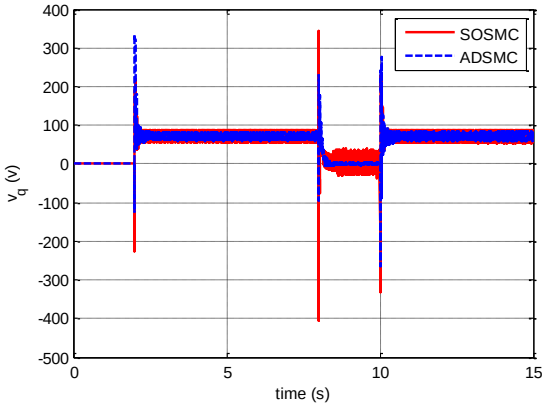

Fig. 12 Control signal along the q-axis in d-q coordinates by applying ADSMC and SOSMC.

5 Conclusions

In this paper, an adaptive dynamic sliding mode controller was used to control active and reactive power for a Brushless DFIG wind turbines. The proposed method is a non-linear control strategy and due to dynamic characteristics it offers a smooth control signal. Moreover, this makes implementation of the controller easier unlike the conventional widely used sliding mode control. The proposed controller is not independent to uncertainty bound due to use adaptive switching gains. Furthermore, simulation results show that the proposed controller generates a smoother control signal compared to the conventional SMC and has lower overshoots compared to the PID and SOSMC methods. In addition, the control signal of the proposed controller has significantly lower maximum amplitude compared to the PID and SOSMC method, particularly at the starting point of control system and after the occurrence and elimination of the voltage dip.

Intellectual Property

The authors confirm that they have given due consideration to the protection of intellectual property associated with this work and that there are no impediments to publication, including the timing to publication, with respect to intellectual property.

Funding

No funding was received for this work.

CRediT Authorship Contribution Statement

M. Ehsani: Idea & Conceptualization, Research & Investigation, Software and Simulation, Original Draft Preparation. **As. Oraee:** Idea & Conceptualization, Supervision, Verification, Revise & Editing. **B. Abdi:** Supervision. **V.**

Behnamgol: Software and Simulation, Supervision, Verification. **S. M. Hakimi:** Supervision.

Declaration of Competing Interest

The authors hereby confirm that the submitted manuscript is an original work and has not been published so far, is not under consideration for publication by any other journal and will not be submitted to any other journal until the decision will be made by this journal. All authors have approved the manuscript and agree with its submission to "Iranian Journal of Electrical and Electronic Engineering".

References

[1] O. Moussa, R. Abdessemed, S. Benaggoune, "Super twisting sliding mode control for brushless doubly fed induction generator based on WECS," *International Journal of System Assurance Engineering and Management*, Vol. 10, No. 5, pp. 1145-1157, 2019.

[2] R. Zhao, A. Zhang, Y. Ma, W. Jia, and Yun Ma "The Dynamic Control of Reactive Power for the Brushless Doubly Fed Induction Machine with Indirect Stator-Quantities Control Scheme," *IEEE Trans Power Electronics*, Vol. 30, No. 9, pp. 5046-5057, 2015.

[3] V. Behnamgol, and A. R. Vali, "Terminal Sliding Mode Control for Nonlinear Systems with both Matched and Unmatched Uncertainties," *Iranian Journal of Electrical and Electronic Engineering*, Vol. 11, No. 2, pp. 109-117, 2015.

[4] G. Zhang, J. Yang, Y. Sun, M. Su, W. Tang, Q. Zhu, and H. Wang, "A robust control scheme based on ISMC for the brushless doubly fed induction machine". *IEEE Transactions on Power Electronics*, Vol. 33, No. 4, pp. 3129-3140, 2017.

[5] X. Yan, M. Cheng, L. Xu, and Y. Zeng, "Dual-Objective Control Using an SMC-Based CW Current Controller for Cascaded Brushless Doubly Fed Induction Generator," *IEEE Transactions on Industry Applications*, Vol. 56, No. 6, pp. 7109-7120, 2020.

[6] D. Zhang, Y. Chen, J. Su, and Y. Kang, "Dual-Mode Control for Brushless Doubly Fed Induction Generation System based on Control-Winding-Current Orientation," *IEEE Journal of Emerging and Selected Topics in Power Electronics*, Vol. 9, No. 2, 2019.

[7] D. Tchioffo, A. K. Fankem, E. D., Golam, G. et al. "Control of a BDFIG Based on Current and Sliding Mode Predictive Approaches," *Journal of Control, Automation and Electrical Systems*, Vol. 31, pp. 636-647, 2020.

[8] P. Li, L. Xiong, F. Wu, M. Ma, and J. Wang, "Sliding mode controller based on feedback linearization for damping of sub synchronous control interaction in DFIG based wind power plants," *International journal of electrical power & energy system*, Vol. 107, pp. 239-250, 2019.

[9] V. Ghaffari, "A Novel Approach to Designing of Chattering-Free Sliding-Mode Control in Second-Order Discrete-Time Systems," *Iranian Journal of Electrical and Electronic Engineering*, Vol. 15, No. 4, pp. 453-461, 2019.

[10] M. Mbukani, and N. Gule, "Comparison of high-order and second-order sliding mode observer based estimators for speed sensorless control of rotor-tied DFIG systems," *IET Power Electronics*, Vol. 12, No. 12, pp. 3231-3241, 2019.

[11] X. Yan, and M. Cheng, "A Robustness—Improved Control Method Based on ST-SMC for Cascaded Brushless Doubly Fed Induction Generator," *IEEE Transactions on Industrial Electronics*, Vol. 68, No. 8, pp. 7061-7071, 2020.

[12] J. Fei, and Y. Chen, "Dynamic Terminal Sliding-Mode Control for Single-Phase Active Power Filter Using New Feedback Recurrent Neural Network," *IEEE Transactions on Power Electronics*, Vol. 35, No. 9, pp. 9904-9922, 2020.

[13] S. Chen, and S. Gong "Speed tracking control of pneumatic motor servo systems using observation-based adaptive dynamic sliding-mode control," *Mechanical Systems and Signal Processing*, Vol. 94, pp. 111-128, 2017.

[14] M. Shokoohinia, M. Fateh, and R. Gholipour, "Design of an adaptive dynamic sliding mode control approach for robotic systems via uncertainty estimators with exponential convergence rate," *SN Applied Sciences*, Vol. 180, No. 2, 2020.

[15] M. Herrera, O. Camacho, and H. Smith, "An approach of dynamic sliding mode control for chemical processes," *Journal of Process Control*, Vol. 85, pp. 112-120, 2020.

[16] Y. Chen, and J. Fei, "Dynamic Sliding Mode Control of Active Power Filter With Integral Switching Gain," *IEEE Access*, Vol. 7, pp. 21635-21644, 2019.

[17] A. Karami, and A. Mollaee, H. Tirandaz, O. Barambones, "On dynamic sliding mode control of nonlinear fractional-order systems using sliding observer," *Nonlinear Dynamics*, Vol. 92, 2018.

[18] R. Hu, H. Deng, and Y. Zhang, "Novel Dynamic-Sliding-Mode-Manifold-Based Continuous Fractional-Order Nonsingular Terminal Sliding Mode Control for a Class of Second-Order Nonlinear Systems," *IEEE Access*, Vol. 8, pp. 19820-19829, 2020.

[19] J. Wang, W. Luo, J. Liu, and L. Wu, "Adaptive Type-2 FNN-Based Dynamic Sliding Mode Control of DC-DC Boost Converters," *IEEE Transactions on Systems, Man, and Cybernetics: Systems*, Vol. 51, No. 4, pp. 2246-2257, 2019.

[20] A. Rauf, S. Li, R. Madonski, and J.Yang, "Continuous dynamic sliding mode control of converter-fed DC motor system with high order mismatched disturbance compensation," *Transactions of the Institute of Measurement and Control*, Vol. 42, No. 14, pp. 2812-2821, 2020.

[21] Y. Hu, and H. Wang , "Robust tracking control for vehicle electronic throttle using adaptive dynamic sliding mode and extended state observer," *Mechanical Systems and Signal Processing*, Vol. 135 ,2020,

[22] S. Roy, S. Baldi, L. M. Fridman, "On adaptive sliding mode control without a priori bounded uncertainty," *Automatica*, Vol. 111, 2020, 108650.

[23] J. Guo, "Application of a novel adaptive sliding mode control method to the load frequency control," *European Journal of Control*, Vol. 57, pp. 172-178, 2021.

[24] J. Zhang et al., "Adaptive Sliding Mode-Based Lateral Stability Control of Steer-by-Wire Vehicles With Experimental Validations," *IEEE Transactions on Vehicular Technology*, Vol. 69, No. 9, pp. 9589-9600, 2020.

[25] F. Plestan, Y. Shtessel, V. Brégeault, and A. Poznyak, "New methodologies for adaptive sliding mode control", *International Journal of Control*, Vol. 83, No. 9, pp. 1907-1919, 2010.

[26] S. Shao, "Control of brushless doubly-fed (induction) machines," Ph.D. dissertation, Dept. Eng., Univ. Cambridge, Cambridge, U.K., 2010.

[27] V. Behnamgol, A. R. Vali, A. Mohammadi, and A. Oraee, "Lyapunov-based Adaptive Smooth Second order Sliding Mode Guidance Law with Proving Finite Time Stability," *Journal of Space Science and Technology*, Vol. 11, No. 2, pp. 33-39, 2018.

[28] J .Liu, and X .Wang, *Advanced sliding mode control for mechanical systems*, Berlin, Springer, 2012.

M. Ehsani was born in Iran in 1985. He received the B.S. degree in electrical engineering from Shomal University, Iran, in 2009, and the M.S. degrees in control engineering from Islamic Azad University, Damavand, Iran, in 2017. He is currently a Ph.D. student in control engineering in Islamic Azad University, Damavand, Iran, since 2017. His research interests include sliding mode and robust control and electrical machines for renewable power generation.

A.Oraee received the B.Eng. degree from Kings College London, London, U.K in 2011.She then completed her Ph.D degree in electrical machine design and modeling from Cambridge University, Cambridge, U.K in 2015. She is currently an Assistant Professor in Electrical Engineering at the University of Sadjad, Iran. Her main research interests include electrical machines and drives for renewable power generation and automotive applications.

B. Abdi received the M.Sc. and Ph.D. degrees from the Amir Kabir University of technology Tehran, Iran, in 2005 and 2010, all in electrical engineering. He was an Assistant Professor with the Damavand University, Damavand, Iran. His research interests include Reliability, Renewable energy and machine designing.

V. Behnamgol was born in Iran in 1985. He received the B.S. degree in electrical engineering from Shomal University, Iran, in 2009, and the M.S. and Ph.D. degrees in control engineering from Malek Ashtar University, Tehran, Iran, in 2011, and 2016. He is currently an assistant professor of Control department at the Malek Ashtar University of Technology of Tehran, Iran. He has authored more than 50 scientific journal and conference papers. His research interests include nonlinear, sliding mode and robust control and guidance systems.

S. M. Hakimi received the B.Sc. degree from the Shiraz University, Iran, in 2004, and the M.Sc. and Ph.D. degrees from the K.N.Toosi University of technology Tehran, Iran, in 2007 and 2014, all in electrical engineering. He is an Assistant Professor with the Damavand University, Damavand, Iran, from 2014 to now. His current research interests include smart grid, Renewable energy, Demand response and IoT.